



XXIV Italian Group of Fracture Conference, 1-3 March 2017, Urbino, Italy

Additively Manufactured PLA under static loading: strength/cracking behaviour vs. deposition angle

A. A. Ahmed^a, L. Susmel^{a,*}

^aDepartment of Civil and Structural Engineering, the University of Sheffield, Mappin Street, Sheffield S1 3JD, UK

Abstract

This paper aims to assess the existing interactions between strength/fracture behaviour and infill angle in additively manufactured PLA subjected to static loading. Plain specimens and samples containing crack-like notches of 3D-printed PLA were manufactured horizontally by making the deposition angle vary from 0° to 90°. A direct inspection of the fracture surfaces revealed that, irrespective of the infill orientation, static failures were caused by two mechanisms, i.e.: (i) initial shear-stress-governed de-bonding between adjacent filaments and subsequent normal-stress-governed breakage of the filaments themselves. The results being generated demonstrate that, from an engineering point of view, the influence of the deposition angle on the overall strength/fracture resistance of additively manufactured PLA can be neglected with little loss of accuracy. The profile of the stress vs. strain curves being obtained experimentally suggests also that the mechanical behaviour of the 3D-printed PLA being investigated can be modelled accurately without requiring the use of complex non-linear material models, with this resulting in a great simplification of the design problem.

Copyright © 2017 The Authors. Published by Elsevier B.V. This is an open access article under the CC BY-NC-ND license (<http://creativecommons.org/licenses/by-nc-nd/4.0/>).

Peer-review under responsibility of the Scientific Committee of IGF Ex-Co.

Keywords: Additive Manufacturing, PLA, deposition angle, static loading, strength, fracture resistance

1. Introduction

Additive Manufacturing (AM) allows objects from three-dimensional numerical models to be fabricated by joining materials layer upon layer. Therefore, AM is an “additive” process that permits components having complex shape to

* Corresponding author. Tel.: +44-(0)114-2225073; fax: +44-(0)114-2225700.
E-mail address: l.susmel@sheffield.ac.uk

Nomenclature

a	notch depth
t	thickness
w _g	gross width
w _n	net width
E	Young's modulus
K _C	fracture toughness
α	shape factor
θ _p	angle defining the manufacturing direction
σ _{0.2%}	0.2% proof stress
σ _F	nominal failure stress referred to the gross area
σ _{UTS}	ultimate tensile strength

be manufactured in a more effective way than conventional “subtractive” technologies, with this being done by reaching a remarkable level of accuracy in terms of both shape and dimensions.

Plastics can be additively manufactured from powders, wires and flat sheets that are melted using a variety of different technologies. Compared to the large variety of plastic materials that can be manufactured by adopting conventional processes, a limited numbers of plastics can be additively manufactured effectively, with acrylonitrile butadiene styrene (ABS) and polylactide (PLA) being the most commonly employed polymers. Other plastic materials such as polyphenyl sulfone and polycarbonate can also be additively manufactured, even though the fabrication processes being required are based on more sophisticated technological solutions.

PLA is a biodegradable, absorbable and biocompatible polymer that is used to manufacture a variety of components/objects that include, amongst other, biomedical devices (Hamad et al., 2015). One of the most important features of PLA is that it can be additively manufactured very easily by using low-cost commercial 3D-printers.

Examination of the state of the art shows that the mechanical properties of additively manufactured PLA are markedly affected by different technological variables such as: nozzle size, layer thickness, infill percentage, filling pattern, filling speed, and manufacturing temperature (de Ciurana et al., 2013; Fernandez-Vicente et al., 2016). It is interesting to observe that other parameters as well are seen to play an important role during the manufacturing process: for instance, given the basic chemical composition of the material being used, pigments affect not only its mechanical properties, but also its level of crystallinity (Wittbrodt and Pearce, 2015).

In this context, certainly the infill orientation is one of the most important variables affecting the overall mechanical, strength, and fracture behaviour of additively manufactured plastics. In particular, by testing unidirectional fused deposition specimens of both PLA and ABS, Lanzotti et al. (2015) have observed that the material ultimate tensile strength decreases by 50% as the infill angle varies from 0° to 90°. Further, on average, the strength along the vertical direction (i.e., along a direction perpendicular to the build-plate) is seen to be about 30% lower than the strength that is obtained along horizontal directions.

From a structural integrity view point, the fact that 3D-printed components can contain very complex geometrical features results in localised stress concentration phenomena, with stress raisers reducing markedly the overall strength of the components themselves (Susmel & Taylor, 2008a, 2008b, 2010; Yin et al., 2015). Accordingly, accurate and simple design techniques are required in order to perform the static assessment of 3D-printed materials accurately.

In this challenging scenario, the aim of the present paper is to investigate whether, under static loading, the deposition angle influences not only the static strength, but also the fracture resistance of additively manufactured PLA.

2. Fabrication of the specimens

Via 3D-printer Ultimaker 2 Extended+, both plain specimens and samples containing crack-like notches were additively manufactured using as parent material white filaments of New Verbatim PLA having diameter equal to

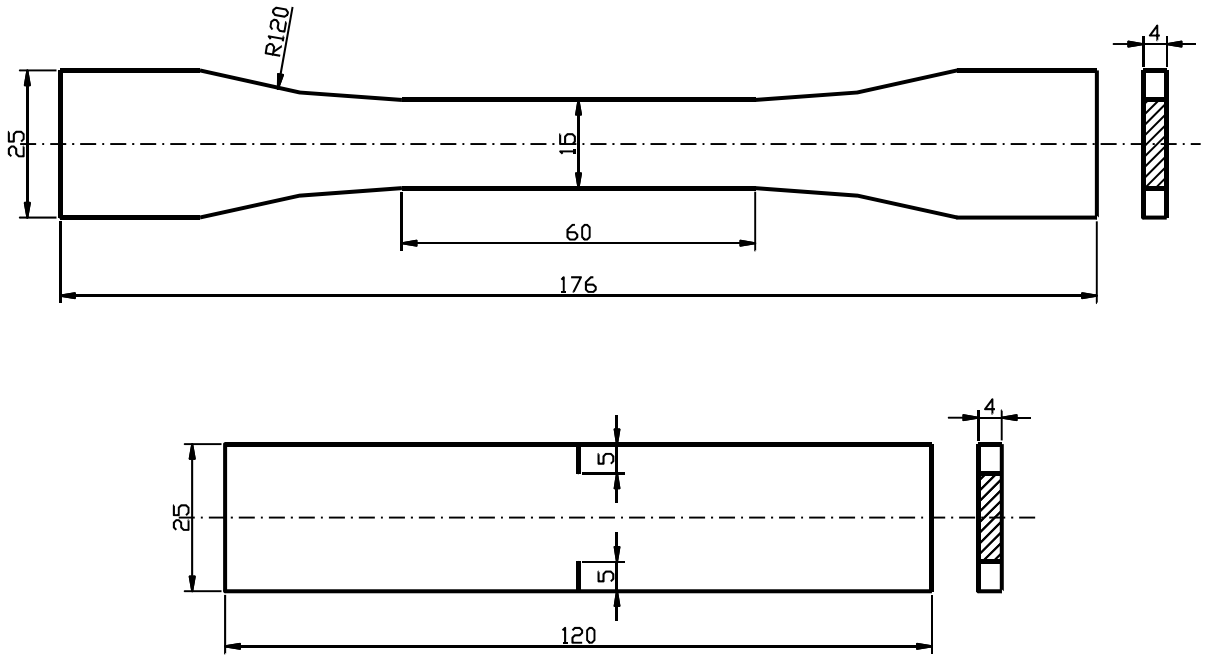


Fig. 1. Geometries of the tested specimens (nominal dimensions in millimetres).

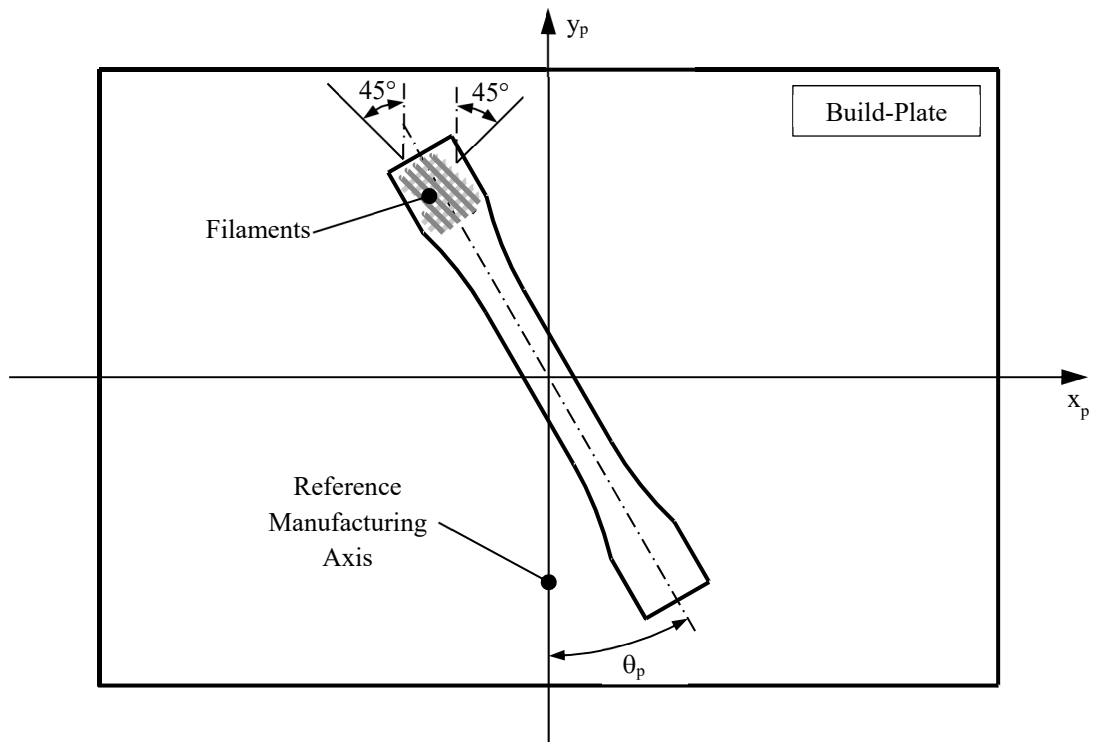


Fig. 2. Manufacturing direction and orientation of the deposition filaments.

2.85mm. The key manufacturing parameters were set as follows: nozzle size=0.4mm, nozzle temperature=240°C, build-plate temperature=60°C, layer height=0.1 mm, shell thickness=0.4mm, fill density=100%, and print speed=30mm/s.

Figure 1 shows the technical drawings of the specimens that were manufactured to investigate experimentally both the static strength and the fracture resistance of the additively manufactured PLA being considered.

The specimens were manufactured horizontally by setting the manufacturing angle, θ_p , equal to 0°, 30°, 45°, 60°, and 90° (Fig. 2). In particular, after melting the parent material filaments, they were extruded and deposited, layer upon layer, at $\pm 45^\circ$ to the reference manufacturing direction, with θ_p being the angle between the reference manufacturing direction and the longitudinal axis of the specimens (see Figure 2).

Table 1. Summary of the experimental results generated by testing plain specimens of AM PLA.

Code	θ_p [°]	w_n [mm]	t [mm]	E [MPa]	$\sigma_{0.2\%}$ [MPa]	σ_{UTS} [MPa]
P_0_2	0	14.95	4.08	3189	40.9	41.5
P_0_3	0	14.93	4.07	3265	42.2	43.1
P_0_4	0	14.97	4.21	3251	42.0	43.4
P_30_1	30	14.85	4.11	3136	35.1	37.7
P_30_2	30	15.09	4.11	3450	40.1	40.8
P_30_3	30	14.92	4.04	3357	40.3	44.2
P_45_1	45	14.87	4.09	3426	38.6	42.9
P_45_2	45	15.15	4.07	3342	40.7	42.5
P_45_3	45	15.03	4.04	3348	39.1	42.1
P_60_1	60	15.06	4.13	3180	-	39.6
P_60_2	60	15.06	4.18	3251	40.1	40.9
P_60_3	60	15.00	4.08	3235	40.1	42.1
P_90_1	90	15.16	3.99	3421	42.4	46.5
P_90_2	90	14.95	3.98	3399	42.3	48.0
P_90_3	90	15.10	4.15	3193	40.7	42.8

Table 2. Summary of the experimental results generated by testing specimens of AM PLA containing crack-like notches.

Code	θ_p [°]	w_g [mm]	t [mm]	a [mm]	α	σ_r [MPa]	K_c [MPa·m ^{1/2}]
C_0_1	0	25.03	4.22	4.67	1.131	28.4	3.9
C_0_2	0	24.78	4.20	4.47	1.130	27.6	3.7
C_0_3	0	24.73	4.22	4.34	1.129	28.0	3.7
C_30_1	30	24.98	4.21	4.86	1.134	21.0	2.9
C_30_2	30	24.98	4.18	4.73	1.132	18.9	2.6
C_30_3	30	24.92	4.18	4.75	1.133	21.2	2.9
C_45_1	45	24.93	4.16	4.72	1.132	23.0	3.2
C_45_2	45	24.90	4.18	4.90	1.134	21.8	3.1
C_45_3	45	24.88	4.16	4.85	1.134	21.4	3.0
C_60_1	60	24.83	4.18	4.63	1.131	20.6	2.8
C_60_2	60	24.80	4.14	4.83	1.134	19.7	2.8
C_60_3	60	24.82	4.08	4.78	1.133	20.5	2.9
C_90_1	90	25.06	4.04	4.75	1.132	25.8	3.6
C_90_2	90	25.06	4.11	5.39	1.142	25.2	3.8
C_90_3	90	24.74	4.08	4.89	1.135	28.4	4.0

Both the plain samples and the specimens containing crack-like notches had thickness equal to 4mm. Crack-like notches were fabricated by cutting the material via a sharp thin knife, with this simple manufacturing process resulting in an average length of the notch root radius equal to about 0.05mm. Tables 1 and 2 summarise, for each specimen being tested, the actual dimensions that were measured using a high-precision calliper as well as an optical microscope. By contrasting the actual dimensions reported in Tables 1 and 2 with the nominal dimensions indicated in Figure 1, it is possible to conclude that the accuracy in terms of dimensions was slightly affected by manufacturing angle θ_p .

3. Static testing

The plain specimens as well as the samples containing crack-like notches manufactured according to the procedure described in the previous section were tested under quasi-static tensile loading by using a Shimadzu universal machine (Fig. 3). During testing, the displacement rate was kept constant and equal to 2 mm/min. In the plain specimens, local strains were measured by employing a standard axial extensometer having gauge length equal to 50 mm (Fig. 3a). Irrespective of the specimen geometry being investigated, the tests were run up to the complete failure (i.e. separation) of the samples. Three different specimens were tested for any geometry/manufacturing configuration being considered.

The results generated by testing the plain samples are summarised in Table 1 in terms of Young's modulus, E , 0.2% proof stress, $\sigma_{0.2\%}$, and ultimate tensile strength, σ_{UTS} .

The results obtained by testing specimens with crack-like notches are reported in Table 2 in terms of fracture toughness for a thickness of 4 mm, K_C . In particular, K_C was estimated by using the following well-known relationship (Anderson, 2005):

$$K_C = \alpha \cdot \sigma_f \cdot \sqrt{\pi a} \quad (1)$$

where α is the shape factor, σ_f is the nominal failure stress referred to the gross area, and a is the crack-like notch depth. To conclude, it is worth observing that the values for the shape factor listed in Table 2 were calculated from the actual dimensions being measured via the following standard formula (Tada et al., 2000):

$$\alpha = 1.122 + 0.203 \cdot \left(\frac{2a}{w_g}\right) - 1.196 \cdot \left(\frac{2a}{w_g}\right)^2 + 1.93 \cdot \left(\frac{2a}{w_g}\right)^3 \quad (2)$$



Fig. 3. Static testing: (a) plain specimens and extensometer; (b) specimen containing two lateral crack-like notches.

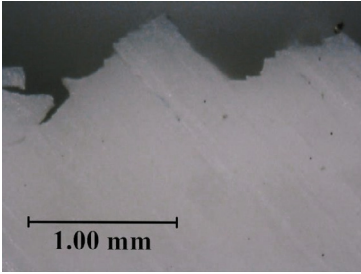
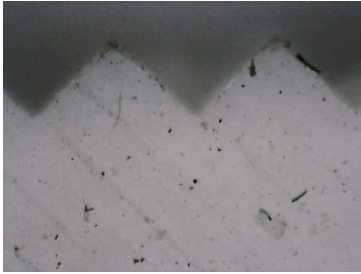
	Plain specimens	Specimens with crack-like notches
$\theta_p=0^\circ$		
$\theta_p=30^\circ$		
$\theta_p=45^\circ$		
$\theta_p=60^\circ$		
$\theta_p=90^\circ$		

Fig. 4. Examples of the cracking behaviour displayed by the specimens being tested (in the different figures the longitudinal axis of the specimens is vertical).

4. Cracking behaviour

The pictures reported in Figure 4 show some examples of the cracking behaviour displayed by the material being tested. In particular, it was seen that, both in the absence and in the presence of stress concentration phenomena, final breakage was due to two different cracking mechanisms, that is: an initial shear-stress-dominated de-bonding between adjacent filaments followed by a normal-stress-governed rectilinear cracking of the filaments themselves.

5. Stress vs. strain behaviour and mechanical properties under static loading

The stress vs. strain diagrams reported in Figure 5 summarise the mechanical behaviour as measured using the plain specimens shown in Figure 1. These diagrams make it evident that in the samples manufactured by setting θ_p equal to 0° (Fig. 5a) as well as to 90° (Fig. 5e) the final failures were all preceded by a quite remarkable elongation. In contrast, for the specimens manufactured by setting θ_p equal to 30° (Fig. 5b), to 45° (Fig. 5c), and to 60° (Fig. 5d), it is seen that the static failures took place as soon as the stress in the recorded stress vs. strain curves reached its maximum value.

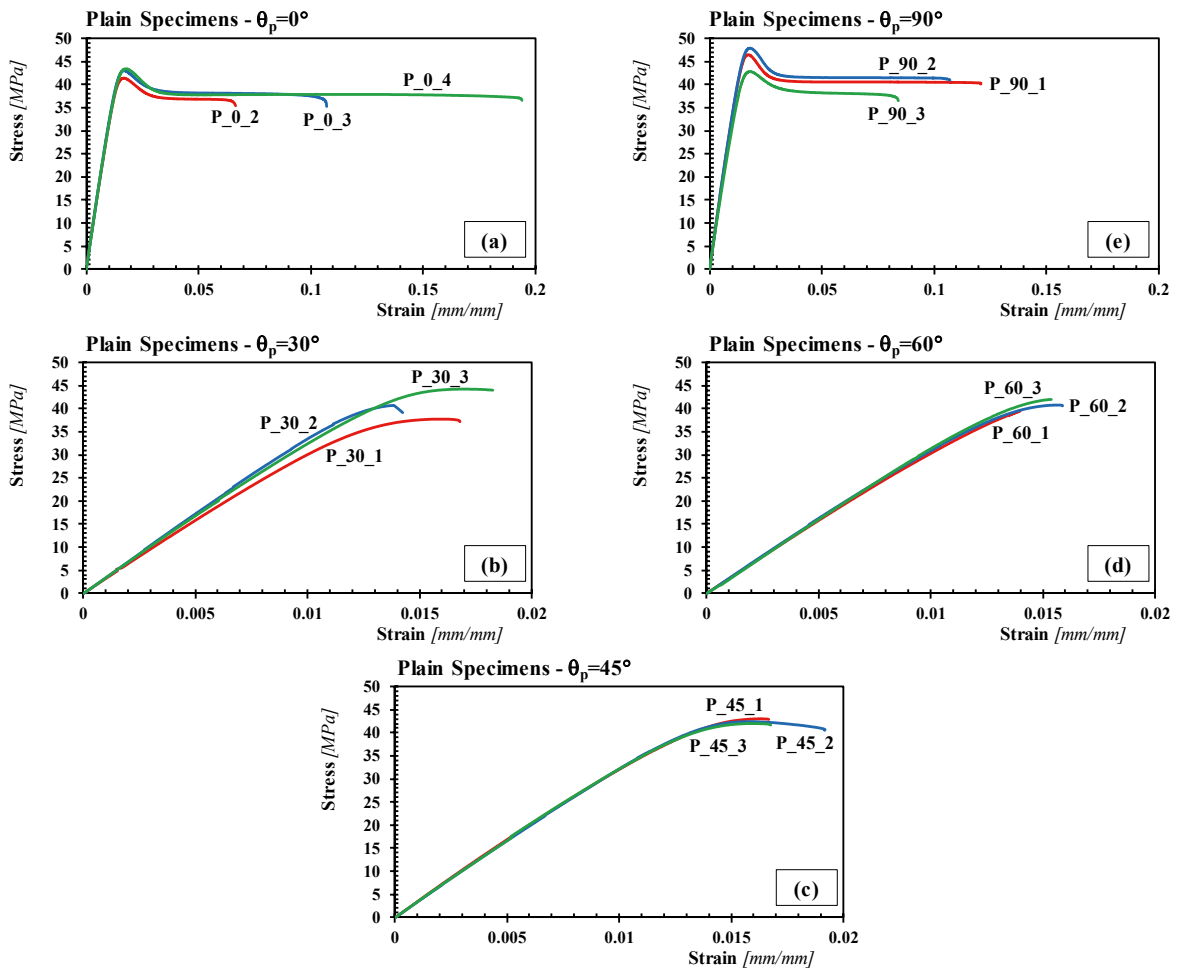


Fig. 5. Experimental stress vs. strain curves generated by testing plain samples manufactured by adopting different values for manufacturing angle θ_p .

In order to investigate the characteristics of the additively manufactured PLA being tested in terms of E , $\sigma_{0.2\%}$ and σ_{UTS} , the charts of Figure 6 plot the values experimentally determined for these mechanical properties against manufacturing angle θ_p (see also Table 1). These diagrams clearly demonstrate that θ_p had little influence on the values measured for E , $\sigma_{0.2\%}$ and σ_{UTS} . In particular, according to Table 1, these material properties averaged from the 15 tests being run were as follows: $E=3296$ MPa, $\sigma_{0.2\%}=40.3$ MPa, and $\sigma_{UTS}=42.5$ MPa. The charts of Figure 6 show that the results generated by making deposition angle θ_p vary in the range 0° - 90° fall within an error interval of $\pm 2S_D$, where S_D is the standard deviation associated with any of the above material mechanical properties.

The diagrams of Figure 5 suggest also that the mechanical behaviour of the additively manufactured polymer under investigation can be assumed to be linear up to the maximum stress value in the recorded stress vs. strain curves. The validity of these assumption is supported also by the fact that the difference between the average value of $\sigma_{0.2\%}$ and the average value of σ_{UTS} was measured to be lower than 1%. Accordingly, in situations of practical interest, the mechanical behaviour of this additively manufactured PLA can be modelled effectively without invoking the use of complex non-linear material constitutive laws.

According to the considerations reported in the previous paragraphs, the conclusion can be drawn that, in the additively manufactured polymer being tested, the mechanical behaviour (and in particular the elongation) in the incipient failure condition was markedly affected by manufacturing angle θ_p . In contrast, the charts of Figure 6 fully support the idea that, from an engineering point of view, the effect of angle θ_p on E , $\sigma_{0.2\%}$ and σ_{UTS} can be neglected with little loss of accuracy.

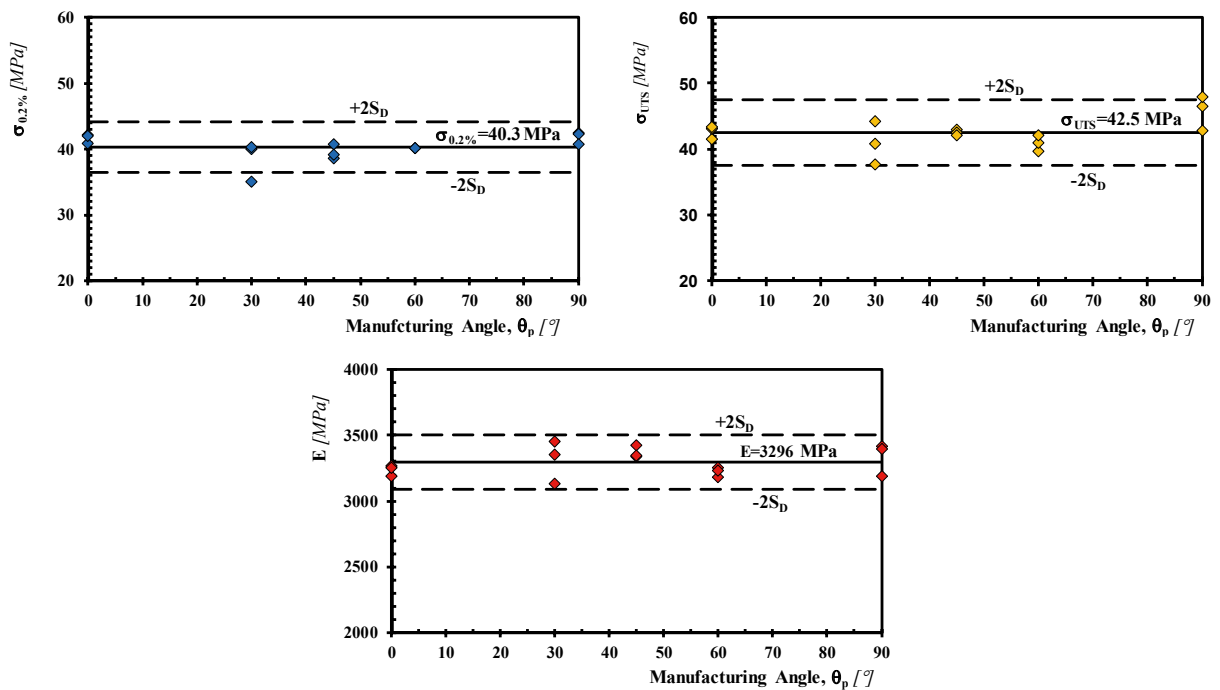


Fig. 6. Influence of manufacturing angle θ_p on $\sigma_{0.2\%}$, σ_{UTS} , and E .

6. Fracture resistance under static loading

The force vs. displacement diagrams reported in Figure 7 summarise the mechanical behaviour displayed by the specimens containing crack-like notches (Fig. 1). As to these charts, it is interesting to observe that, independently of the value of manufacturing angle θ_p , the loading curves all show two linear branches having slightly different slope. This can be ascribed to the fact that the initial deformations were seen to occur predominantly at the interfaces between adjacent filaments. As soon as this initial straining process exhausted itself, the filaments started deforming, with this

change in the straining mechanism resulting in the keen points that are visible in the force vs displacement curves reported in Figure 7.

In terms of fracture toughness determined for $t=4$ mm, the K_{IC} vs. θ_p diagram of Figure 8 shows that the largest K_{IC} values were obtained for θ_p equal to 0° and to 90° , whereas the lowest values for θ_p equal to 30° and to 60° . This suggests that, from a scientific point of view, the fracture toughness of the AM material being investigated is influenced by the manufacturing direction. However, the chart of Figure 8 makes it evident that all the experimental data are within two standard deviations of the mean, with the average value for K_{IC} being equal to $3.2 \text{ MP}\cdot\text{m}^{1/2}$ (see also Table 2). Therefore, from an engineering point of view, the fracture toughness of the additively manufactured polymer being investigated can be assumed, with little loss of accuracy, to be independent from θ_p , with this holding true provided that the material itself is additively manufactured horizontally.

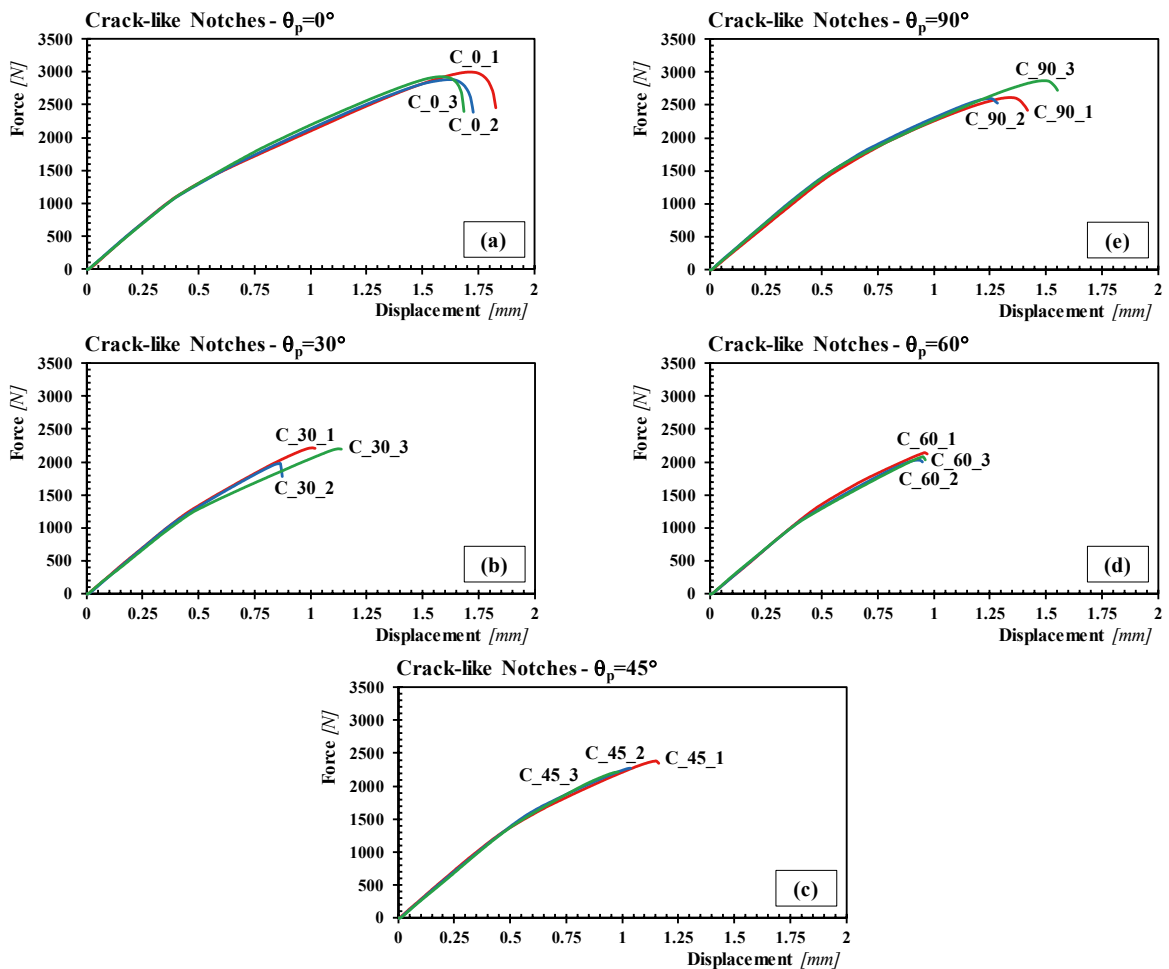


Fig. 7. Experimental force vs. displacement curves generated by testing crack-like notched samples manufactured by adopting different values for manufacturing angle θ_p .

Conclusions

The experimental results summarised in the present paper demonstrate that:

- both the mechanical and the cracking behaviour of the PLA being investigated were not influenced markedly by the fabrication direction, with this holding true provided that the material is additively manufactured horizontally;

- since the stress vs. strain curves generated by testing the plain specimens (Fig. 5) were seen to be all characterised by a remarkable level of linearity up to the ultimate tensile stress, the mechanical behaviour of the investigated 3D-printed PLA can be modelled successfully by directly using a simple linear-elastic constitutive law.

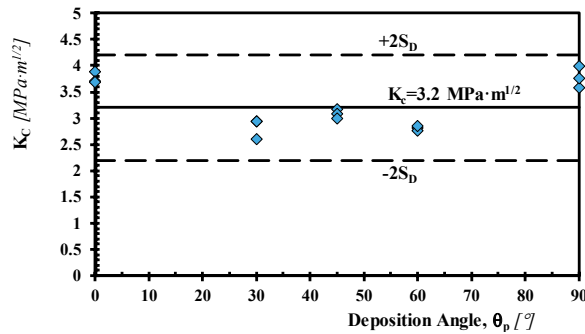


Fig. 8. Influence of manufacturing angle θ_p on K_{IC} .

References

- Anderson, T.L., 2005. Fracture Mechanics: Fundamentals and Applications, CRC Press, USA.
- de Ciurana, J., Serenó, L., Vallès, E., 2013. Selecting Process Parameters in RepRap Additive Manufacturing System for PLA Scaffolds Manufacture. *Procedia CIRP* 5, 152-157.
- Fernandez-Vicente, M., Calle, W., Ferrandiz, S., Conejero, A., 2016. Effect of Infill Parameters on Tensile Mechanical Behavior in Desktop 3D Printing. *3D Printing and Additive Manufacturing* 3(3), 183-192.
- Hamad, K., Kaseem, M., Yang, H.W., Deri, F., Ko, Y.G., 2015. Properties and medical applications of polylactic acid: a review. *eXPRESS Polymer Letters* 9(5), 435–455.
- Lanzotti, A., Grasso, M., Staiano, G., Martorelli, M., 2015. The impact of process parameters on mechanical properties of parts fabricated in PLA with an open-source 3-D printer. *Rapid Prototyping Journal* 21(5), 604-617.
- Susmel, L., Taylor, D., 2008a. The theory of critical distances to predict static strength of notched brittle components subjected to mixed-mode loading. *Engineering Fracture Mechanics* 75(3-4), 534-550.
- Susmel, L., Taylor, D., 2008b. On the use of the Theory of Critical Distances to predict static failures in ductile metallic materials containing different geometrical features. *Engineering Fracture Mechanics* 75, 4410-4421.
- Susmel L., Taylor D., 2010. The Theory of Critical Distances to estimate the static strength of notched samples of Al6082 loaded in combined tension and torsion. Part II: Multiaxial static assessment. *Engineering Fracture Mechanics* 77, 470–478.
- Tada, H., Paris, P.C., Irwin, G.R., 2000. Stress Analysis of Cracks Handbook, ASME Press, USA.
- Yin, T., Tyas, A., Plekhov, O., Terekhina, A., Susmel, L., 2015. A novel reformulation of the Theory of Critical Distances to design notched metals against dynamic loading. *Materials and Design* 69, 197–212.
- Wittbrodt, B., Pearce, J. M., 2015. The effects of PLA color on material properties of 3-D printed components. *Additive Manufacturing* 8, 110-116.